Open Access Library Journal
2022, Volume 9, e9181
ISSN Online: 2333-9721
ISSN Print: 2333-9705

Role of Three Bands on Coexistence of Superconductivity and Antiferromagnetism in Samarium Iron Pnictide Superconductor

Shamin Masih*, Piyush Masih, Sarita Khandka

SHUATS, Prayagraj, India
Email: *shamin.masih@shiats.edu.in, piyush.masih@shiats.edu.in, sarita.khandka@shiats.edu.in

How to cite this paper: Masih, S., Masih, P. and Khandka, S. (2022) Role of Three Bands on Coexistence of Superconductivity and Antiferromagnetism in Samarium Iron Pnictide Superconductor. *Open Access Library Journal*, **9**: e9181.
https://doi.org/10.4236/oalib.1109181

Received: August 4, 2022
Accepted: August 28, 2022
Published: August 31, 2022

Abstract

The coexistence of long range magnetic order and superconductivity in the iron pnictide superconductor $SmFeAsO_{1-x}F_x$ is the basis for the present study that analyses theoretically the role of multiple bands on the coexistence of superconductivity (SC) and antiferromagnetism (AFM). For this, a model Hamiltonian is developed and using Green's function technique, expressions for T_C, T_M and magnetic order parameter η are obtained. For one band, two band and three band models separately, variation of T_C, T_M with η is studied. Further, the coexistence region has been extracted using the above information. The results show that superconducting and AFM order can coexist in this class of superconductors and increasing the number of bands increases the coexistence region.

Subject Areas

Condensed State Physics

Keywords

Superconductivity, Antiferromagnetism, Superconducting Order Parameter, Magnetic Order Parameter

1. Introduction

The iron pnictide superconductors [1] [2] [3] provide promising avenue for research as a lot many features set them apart from known superconductors along with the hitherto high T_C found in this class of superconductors.

Iron pnictides stand second in line after the cuprates [4] to show high T_C of around 55 K [5]. These transition metal based superconductors of the 1111 family having general formula LnOFeAs (Ln = La, Ce, Sm, Gd, Nd, Pr) are layered structures with alternate LnO & FeAs layers, superconductivity believed to be present in the FeAs layers [6]. The atomic structure [7] of the 1111 family consists of negatively charged FeP or FeAs layers, where Fe atoms form a planar square lattice, and positively charged LnO layers, The structure orientation of Fe atoms shows it to be surrounded by four arsenic atoms resulting in a distorted tetrahedral geometry. The iron atoms are seen to make a square lattice and arsenic atoms are placed at the centre of each square being displaced above & below the Fe planes. It has been shown that in the normal state, these compounds are semi-metals [8] (upon doping [9] or application of pressure [10] [11] [12] [13] is seen to increase T_C in iron pnictides). Angle resolved photoemission experiments [14] have demonstrated that iron pnictides are multiband [15] [16] in nature. Iron has five bands at the Fermi surface and all the five d-bands of iron are relevant in studying the superconducting properties of these compounds. Previous theories have found that multiband nature [17] of iron pnictides makes them a significant class in the vast area of superconductivity and that multiband superconductivity serves as an important ingredient for high T_C for this class of compounds. The four unpaired d electrons of iron are seen to hybridise [18] with the three unpaired p electrons of arsenic, resulting in bands found at the Fermi surface due to overlapping orbitals [19] [20]. Raghu [21] *et al.* has discussed a minimal two band model [22] [23] is needed for the superconducting iron pnictides. Two band BCS superconductivity is studied by Maksimov [24] *et al.* for the compound $Ba(Fe_{0.9}CO_{0.1})_2As_2$. Three band superconductivity [25] [26] [27] is also studied and Ummarino [28] has suggested that a simple three band model in strong-coupling regime can reproduce in a quantitative way the experimental T_C. Thus the multiband property of these compounds helps in better understanding of these materials.

Another feature that has created a lot of interest among researchers is the coexistence of superconductivity and magnetism [29] [30] [31] [32] in these superconductors. Extensive experimentation is carried out in various compounds [33] that has shown both the superconducting order parameter and the magnetic order parameter to coexist [34] [35] simultaneously. Theoretical study based on single band model [36] has been carried by Abera Mebrahtu *et al.* showing coexistence of superconductivity and AFM in $SmAsO_{1-x}F_xFe$. Also the interplay of superconductivity and magnetism in FeAs based superconductors is studied theoretically [37] by Mesfin A. Afrassa *et al.* Some other theoretical studies include coexistence of superconductivity and spin density wave in ferropnictide $Ba_{1-x}K_xFe_2As_2$ [38], the coexistence of superconductivity and ferromagnetism [39] and coexistence of superconducting and magnetic order in one band and two band SmOFeAs superconductor [40].

In view of the above, the present theoretical work aims to explore the role of multiband SmOFeAs superconductor. In this work, using Green's function technique [41], we have studied coexistence of the two orders for one band, two band and three band models and to understand the behaviour of the two orders existing simultaneously. Expressions for T_C, T_M and η are obtained as a function of the number of bands and the coexistence region is extracted from them.

2. Theoretical Model System Hamiltonian

The model Hamiltonian for study of magnetic properties using both localized and itinerant nature of electrons is written as:

$$\begin{aligned} H = {} & \sum_{mk\sigma} E_{mk\sigma} a^{+}_{mk\sigma} a_{mk\sigma} + \sum_{p\sigma} E_{p\sigma} b^{+}_{p\sigma} b_{p\sigma} - \sum_{mkk'} V_{BCS} a^{+}_{mk\uparrow} a^{+}_{m-k\downarrow} a_{mk'\downarrow} a_{m-k'\uparrow} \\ & + \sum_{kk'll'} \alpha_{kq} \left(a^{+}_{mk\uparrow} a^{+}_{m-k\downarrow} b_{ml\downarrow} b_{ml',\uparrow} + h.c \right) - \sum_{\substack{kk' \\ m\neq n}} V_{mn} a^{+}_{mk\uparrow} a^{+}_{m-k\downarrow} a_{n-k'\downarrow} a_{nk',\uparrow} \end{aligned} \tag{1}$$

The first term represents energy of itinerant electrons. The second term denotes energy of localised electrons. The third term is the interaction between electron and electron through boson (phonon). The fourth term is the interaction term between conduction electrons and localized electrons due to some unspecified mechanism with coupling constant α. The fifth term represents interband interaction.

Here m, n are the band indices, k is wave vector, σ is spin of fermions and p is site index for localized electrons. Operator 'a' is for conduction electrons and operator 'b' is for localized electrons.

Coexistence of Superconductivity and Antiferromagnetism

In this section, magnetic properties of magnetic order parameter and coexistence of superconductivity and magnetism is investigated as a function of the number of bands using Green's function formalism.

Considering the two Green's functions for conduction electrons:

$$G_{\substack{\uparrow\uparrow \\ rsqq}} = \left\langle \left\langle a_{rq\uparrow}, a^{+}_{sq\uparrow} \right\rangle \right\rangle \tag{2a}$$

$$G_{\substack{\downarrow\uparrow \\ rs-qq}} = \left\langle \left\langle a^{+}_{r-q\downarrow}, a^{+}_{sq\uparrow} \right\rangle \right\rangle \tag{2b}$$

Following two equations of motion are obtained:

$$\begin{aligned} & \left(\omega - E_{rq\uparrow} + V_{BCS}\gamma_{\downarrow\downarrow} \right) G_{\substack{rs\uparrow\uparrow \\ qq}} \\ & = \frac{\delta_{rs}}{2\pi} - \left(\Delta_{rr} + \sum_{\substack{n \\ r\neq n}} \Delta_{nn} - n_{rr} \right) G_{\substack{rs\ \downarrow\uparrow \\ -qq}} - \sum_{\substack{n \\ r\neq n}} \gamma_{\downarrow\downarrow} V_{rn} G_{\substack{ns\uparrow\uparrow \\ qq}} \end{aligned} \tag{3}$$

$$\begin{aligned} & \left(\omega + E_{r-q\downarrow} - V_{BCS}\gamma_{\uparrow\uparrow} \right) G_{\substack{\downarrow\uparrow \\ rs-qq}} \\ & = -\left(\Delta_{rr} + \sum_{\substack{m \\ m\neq r}} \frac{V_{mr}}{V_{mm}} \Delta_{mm} - \eta_{rr} \right) G_{\substack{\uparrow\uparrow \\ rsqq}} + \sum_{\substack{m \\ m\neq r}} V_{mr}\gamma_{\uparrow\uparrow} G_{\substack{\downarrow\uparrow \\ ms-qq}} \end{aligned} \tag{4}$$

In the calculations that follow, the following Green's functions are used:

$$G_1 = G_{\substack{\uparrow\uparrow \\ 11qq}}$$

$$G_2 = G_{\substack{\downarrow\uparrow \\ 11-qq}}$$

$$G_3 = G_{\substack{\uparrow\uparrow \\ 12qq}} = G_{\substack{\uparrow\uparrow \\ 21qq}}$$

$$G_4 = G_{\substack{\downarrow\uparrow \\ 12-qq}} = G_{\substack{\downarrow\uparrow \\ 21-qq}}$$

$$G_5 = G_{\substack{\uparrow\uparrow \\ 22qq}}$$

$$G_6 = G_{\substack{\downarrow\uparrow \\ 22-qq}}$$

$$G_7 = G_{\substack{\uparrow\uparrow \\ 23qq}} = G_{\substack{\uparrow\uparrow \\ 32qq}}$$

$$G_8 = G_{\substack{\downarrow\uparrow \\ 23-qq}} = G_{\substack{\downarrow\uparrow \\ 32-qq}}$$

$$G_9 = G_{\substack{\uparrow\uparrow \\ 32qq}}$$

$$G_{10} = G_{\substack{\downarrow\uparrow \\ 33-qq}}$$

Solving for one band model

The superconducting order parameter is defined as:

$$\Delta_{11} = \sum_K V_{11} \left\langle a^+_{1k\uparrow}, a^+_{1-k\downarrow} \right\rangle$$

The correlation function is obtained as:

$$\left\langle a^+_{1k\uparrow}, a^+_{1-k\downarrow} \right\rangle = -\frac{1}{i}\int_{-\infty}^{\infty} \frac{G_2(\omega+i\varepsilon)-G_2(\omega-i\varepsilon)}{e^{\frac{\omega}{KT}}-\eta}$$

$$= \frac{\Delta_{11}-\eta_{11}}{2\sqrt{\left(E_{1q\uparrow}-V_{BCS}\gamma\right)^2+\left(\Delta_{11}-\eta_{11}\right)^2}} \tanh\left(\frac{\sqrt{\left(E_{1q\uparrow}-V_{BCS}\gamma\right)^2+\left(\Delta_{11}-\eta_{11}\right)^2}}{2kT}\right) \quad (5)$$

Solving for two band model

The first correlation function is obtained as:

$$\left\langle a^+_{1k\uparrow}, a^+_{1-k\downarrow} \right\rangle$$

$$= \frac{\frac{V_{12}}{V_{22}}\Delta_{22}+\Delta_{11}-\eta_{11}}{2\sqrt{\left(\frac{V_{12}}{V_{22}}\Delta_{22}+\Delta_{11}-\eta_{11}\right)^2+\left(E_{1q\uparrow}-V_{BCS}\gamma\right)^2}} \tanh\frac{\sqrt{\left(\frac{V_{12}}{V_{22}}\Delta_{22}+\Delta_{11}-\eta_{11}\right)^2+\left(E_{1q\uparrow}-V_{BCS}\gamma\right)^2}}{2kT} \quad (6)$$

The second correlation function is written as:

$$\left\langle a^+_{2k\uparrow}, a^+_{2-k\downarrow} \right\rangle = -\frac{1}{i}\int_{-\infty}^{\infty} \frac{G_6(\omega+i\varepsilon)-G_6(\omega-i\varepsilon)}{e^{\frac{\omega}{KT}}-\eta}$$

$$= \frac{\frac{V_{21}}{V_{11}}\Delta_{11}+\Delta_{22}-\eta_{22}}{2\sqrt{\left(\frac{V_{21}}{V_{11}}\Delta_{11}+\Delta_{22}-\eta_{22}\right)^2+\left(E_{2q\uparrow}-V_{BCS}\gamma\right)^2}} \tanh\frac{\sqrt{\left(\frac{V_{21}}{V_{11}}\Delta_{11}+\Delta_{22}-\eta_{22}\right)^2+\left(E_{2q\uparrow}-V_{BCS}\gamma\right)^2}}{2kT} \quad (7)$$

Solving for three band model

$$\Delta_{11} = \frac{\left(\Delta_{11} + \frac{V_{12}}{V_{22}}\Delta_{22} + \frac{V_{13}}{V_{33}}\Delta_{33} - \eta_{11}\right)\tanh \frac{\sqrt{\left(\Delta_{11} + \frac{V_{12}}{V_{22}}\Delta_{22} + \frac{V_{13}}{V_{33}}\Delta_{33} - \eta_{11}\right)^2 + \left\{E_{1q\uparrow} - V_{BCS}\gamma + \gamma\frac{V_{12}V_{31}}{V_{32}}\right\}^2}}{2kT}}{2\sqrt{\left(\Delta_{11} + \frac{V_{12}}{V_{22}}\Delta_{22} + \frac{V_{13}}{V_{33}}\Delta_{33} - \eta_{11}\right)^2 + \left\{E_{1q\uparrow} - V_{BCS}\gamma + \gamma\frac{V_{12}V_{31}}{V_{32}}\right\}^2}} \tag{8}$$

$$\Delta_{22} = \frac{\left(\frac{V_{21}}{V_{11}}\Delta_{11} + \Delta_{22} + \frac{V_{23}}{V_{33}}\Delta_{33} - \eta_{22}\right)\tanh \frac{\sqrt{\left(E_{2q\uparrow} - V_{BCS}\gamma\right)^2 + \left(\frac{V_{21}}{V_{11}}\Delta_{11} + \Delta_{22} + \frac{V_{23}}{V_{33}}\Delta_{33} - \eta_{22}\right)^2}}{2kT}}{2\sqrt{\left(E_{2q\uparrow} - V_{BCS}\gamma\right)^2 + \left(\frac{V_{21}}{V_{11}}\Delta_{11} + \Delta_{22} + \frac{V_{23}}{V_{33}}\Delta_{33} - \eta_{22}\right)^2}} \tag{9}$$

The third correlation function is:

$$\left\langle a_{3k\uparrow}^{+}, a_{3-k\downarrow}^{+} \right\rangle = \frac{-1}{i}\int_{-\infty}^{\infty} \frac{G_{10}\left(\omega + iE\right) - G_{10}\left(\omega - iE\right)}{\mathrm{e}^{\frac{\omega}{kT}} - \eta}$$

$$\Delta_{33} = \frac{\left(\frac{V_{31}}{V_{11}}\Delta_{11} + \frac{V_{32}}{V_{22}}\Delta_{22} + \Delta_{33} - \eta_{11}\right)\tanh \frac{\sqrt{\left(\frac{V_{31}}{V_{11}}\Delta_{11} + \frac{V_{32}}{V_{22}}\Delta_{22} + \Delta_{33} - \eta_{11}\right)^2 + \left[E_{3q\uparrow} - V_{BCS}\gamma + \gamma\frac{V_{32}V_{13}}{V_{12}}\right]^2}}{2kT}}{2\sqrt{\left(\frac{V_{31}}{V_{11}}\Delta_{11} + \frac{V_{32}}{V_{22}}\Delta_{22} + \Delta_{33} - \eta_{11}\right)^2 + \left[E_{3q\uparrow} - V_{BCS}\gamma + \gamma\frac{V_{32}V_{13}}{V_{12}}\right]^2}} \tag{10}$$

Now considering the two Green's functions for localized electrons:

$$G_{\underset{l'l'}{\uparrow\uparrow}} = \left\langle\left\langle b_{l'\uparrow}, b_{l'\uparrow}^{+} \right\rangle\right\rangle \tag{11a}$$

$$G_{\underset{pl'}{\downarrow\uparrow}} = \left\langle\left\langle b_{p\downarrow}^{+}, b_{l'\uparrow}^{+} \right\rangle\right\rangle \tag{11b}$$

The two equations of motion obtained are:

$$\left(\omega - E_{l'\uparrow}\right)G_1 - \Delta_M G_2 = \frac{1}{2\pi} \tag{12}$$

$$\left(\omega + E_{P\downarrow}\right)G_2 - \Delta_M G_1 = 0 \tag{13}$$

Taking $\Delta_M = \sum_{mp}\alpha\frac{\Delta_{mm}}{V} = \sum_{mp'}\frac{\alpha\Delta_{mm}}{V}$, $G_1 = G_{l'l'}^{\uparrow\uparrow}$ and $G_2 = G_{pl'}^{\downarrow\uparrow}$.

The antiferromagnetic order parameter is defined as:

$$\eta_{rr} = \alpha\sum_{pp'}\left\langle b_{r\uparrow}, b_{r\downarrow} \right\rangle$$

Correlation function is written as:

$$\left\langle b_{r\uparrow}, b_{r\downarrow} \right\rangle = i\int_{-\infty}^{\infty} \frac{G_2\left(\omega + iE\right) - G_2\left(\omega - iE\right)}{\mathrm{e}^{\frac{\omega}{kT}} - 1}$$

Antiferromagnetic order parameter for different number of band models is written as:

$$\eta_{rr} = \frac{\alpha \sum_r \left(\sum_M \frac{\alpha \Delta_{MM}}{V_{MM}} \right)}{2\sqrt{E^2 + \left(\sum_M \frac{\alpha \Delta_{MM}}{V_M} \right)^2}} \tanh \left(\frac{\sqrt{E^2 + \left(\sum_M \frac{\alpha \Delta_{MM}}{V_{MM}} \right)^2}}{2kT} \right) \tag{14}$$

For one band model:

$$\eta_{11} = N_O \alpha \int_0^{\hbar\omega_D} \frac{\alpha \frac{\Delta_{11}}{V_{11}}}{2\sqrt{E^2 + \left(\alpha \frac{\Delta_{11}}{V_{11}} \right)^2}} \tanh \frac{\sqrt{E^2 + \left(\alpha \frac{\Delta_{11}}{V_{11}} \right)^2}}{2kT} \tag{15}$$

For two band model:

$$\eta_{22} = N_O \alpha \int_0^{\hbar\omega_D} \frac{\alpha \frac{\Delta_{11}}{V_{11}} + \frac{\Delta_{22}}{V_{22}}}{2\sqrt{E^2 + \alpha^2 \left(\frac{\Delta_{11}}{V_{11}} + \frac{\Delta_{22}}{V_{22}} \right)^2}} \tanh \frac{\sqrt{E^2 + \alpha^2 \left(\frac{\Delta_{11}}{V_{11}} + \frac{\Delta_{22}}{V_{22}} \right)^2}}{2kT} \tag{16}$$

For three band model:

$$\eta_{33} = N_O \alpha \int_0^{\hbar\omega_D} \frac{\alpha \left(\frac{\Delta_{11}}{V_{11}} + \frac{\Delta_{22}}{V_{22}} + \frac{\Delta_{33}}{V_{33}} \right)}{2\sqrt{E^2 + \alpha^2 \left(\frac{\Delta_{11}}{V_{11}} + \frac{\Delta_{22}}{V_{22}} + \frac{\Delta_{33}}{V_{33}} \right)^2}} \tanh \frac{\sqrt{E^2 + \alpha^2 \left(\frac{\Delta_{11}}{V_{11}} + \frac{\Delta_{22}}{V_{22}} + \frac{\Delta_{33}}{V_{33}} \right)^2}}{2kT} \tag{17}$$

3. Results and Discussion

In this study, T_C, η and T_M for multiband iron pnictides is investigated. The variation of T_C with η and variation of T_M with η are studied to obtain the region where both orders, *i.e.*, superconducting and AFM coexist. The region under the two graphs is merged that shows the coexistence of superconductivity and AFM in the system. The problem is solved keeping in mind the multiband nature of pnictides and expressions are obtained for one band, two band and three band models and solved as a function of the number of bands.

Using Equation (5), the variation of T_C vs η_{11} for one band model is plotted. **Figure 1** indicates that till about 9 K, as η_{11} increases, T_C also increases. After 9 K, η_{11} decreases with increasing T_C. At low T_C, η increases, but beyond a critical T_C of 9 K in the one band model, as T_C increases, in order to stabilise superconductivity, η decreases.

Using Equation (14), the variation of T_M vs η_{11} for one band model is plotted. From this graph, it is observed that η_{11} increases with T_M.

Using **Figure 1** and **Figure 2**, T_C and T_M vs. η_{11} are plotted. The region under the intersection of the two merged graphs demonstrates that superconductivity and AFM coexist in iron pnictides. The area under the curve is found to be 9.44 square units (**Figure 3**).

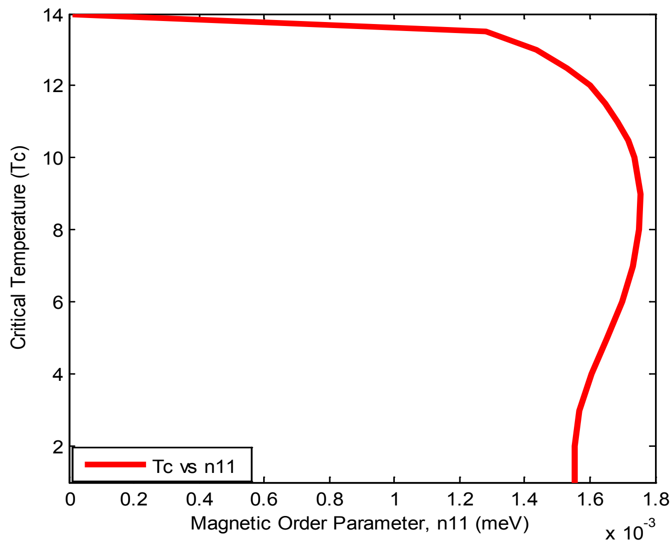

Figure 1. T_C (K) vs η_{11} (meV) for 1 band model.

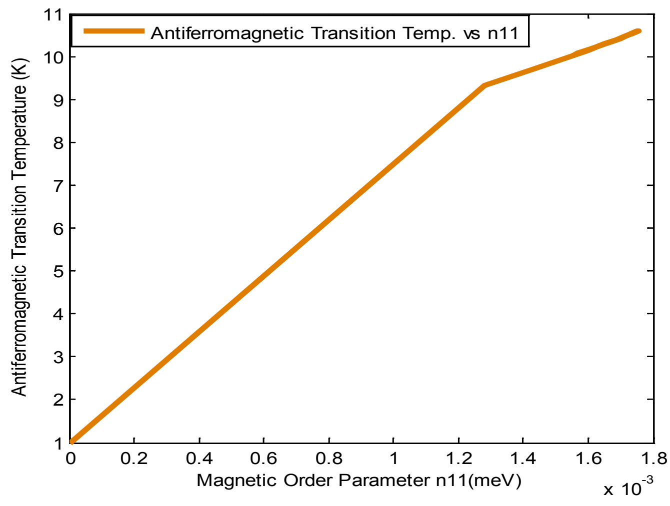

Figure 2. T_M (K) vs η_{11} (meV) for 1 band model.

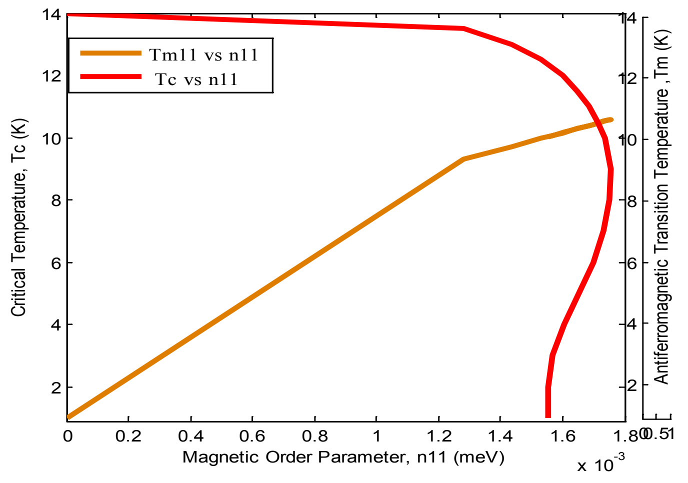

Figure 3. T_C (K) and T_M (K) vs η_{11} (meV) for 1 band model.

Using Equation (6) and (7), the variation of T_C vs η_{22} for two band model is plotted. Figure 4 indicates that till about 35 K, as η_{22} increases, T_C also increases. After 35 K, η_{22} decreases with increasing T_C. At low T_C, η increases, but beyond a critical T_C of 35 K in the two band model, as T_C increases, in order to stabilise superconductivity, η decreases.

Using Equation (15), the variation of T_M vs η_{22} for two band model is plotted. From this graph, it is observed that η_{22} increases with T_M.

Using Figure 4 and Figure 5, T_C and T_M vs. η_{22} are plotted. The region under the intersection of the two merged graphs demonstrates that superconductivity and AFM coexist in iron pnictides. The area under the curve is found to be 36 square units (Figure 6).

Using Equation (8), (9) and (10), the variation of T_C vs η_{33} for 3 band model is plotted. Figure 7 indicates that till about 25 K, as η_{33} increases, T_C also increases. After 25 K, η_{33} decreases with increasing T_C. At low T_C, η increases, but beyond a critical T_C of 25 K in this model, as T_C increases, in order to stabilise superconductivity, η decreases.

Using Equation (16), the variation of T_M vs η_{33} for three band model is plotted. From this graph, it is observed that η_{33} increases with T_M.

Using Figure 7 and Figure 8, T_C and T_M vs. η_{33} are plotted. The region under the intersection of the two merged graphs demonstrates that superconductivity and AFM coexist in iron pnictides. The area under the curve is found to be 70.68 square units.

The present theoretical study, to an extent has been able to explain the coexistence of superconductivity and magnetism in multiband SmOFeAs superconductor. The compound SmOFeAs upon doping is seen to show both superconductivity and magnetic order [42]. Figure 3, Figure 6 and Figure 9 show the coexistence curves for one, two and three band models respectively.

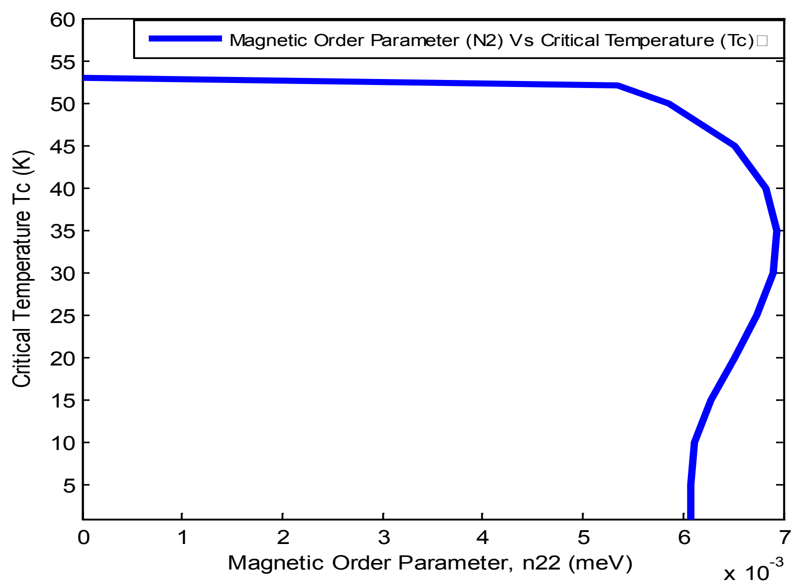

Figure 4. T_C (K) vs η_{22} (meV) for 2 band model.

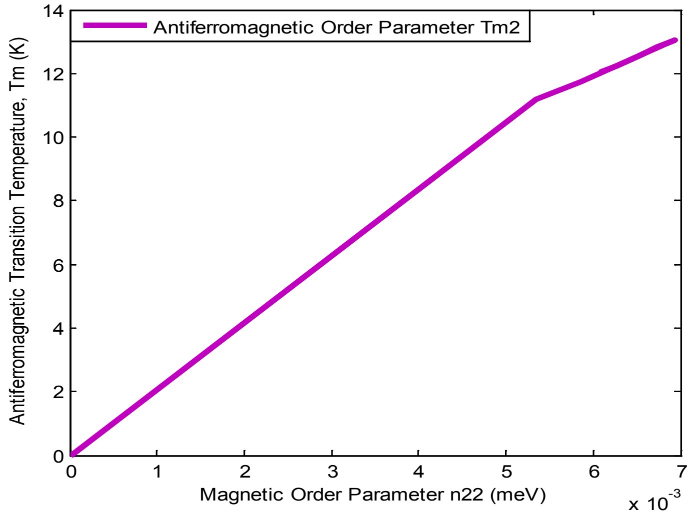

Figure 5. T_M (K) vs η_{22} (meV) for 2 band model.

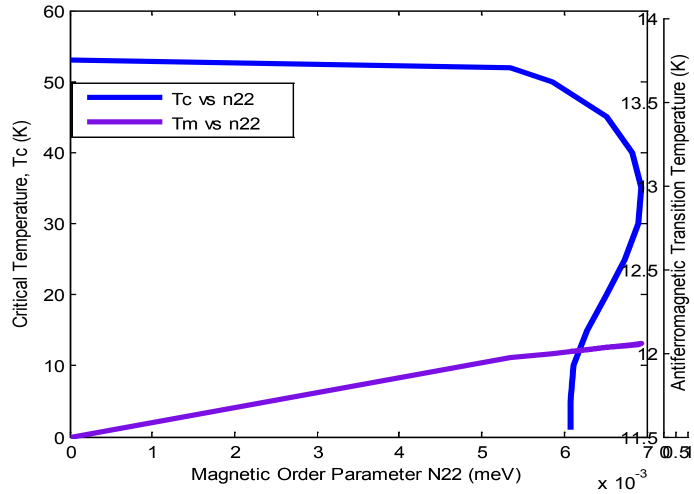

Figure 6. T_C and T_M (K) vs η_{22} (meV) for 2 band model.

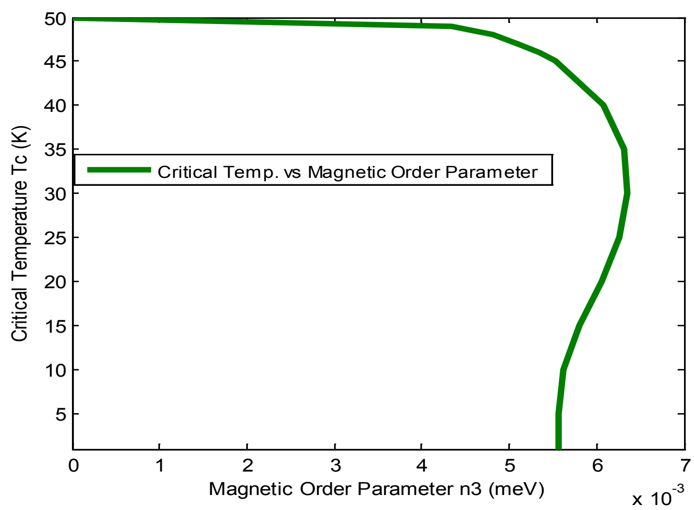

Figure 7. T_C vs η_{33} for 3 band model.

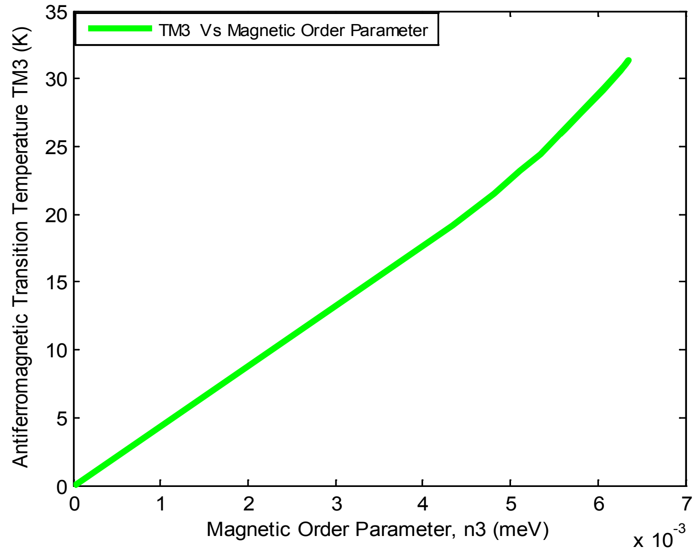

Figure 8. T_M (K) vs η_{33} (meV) for 3 band model.

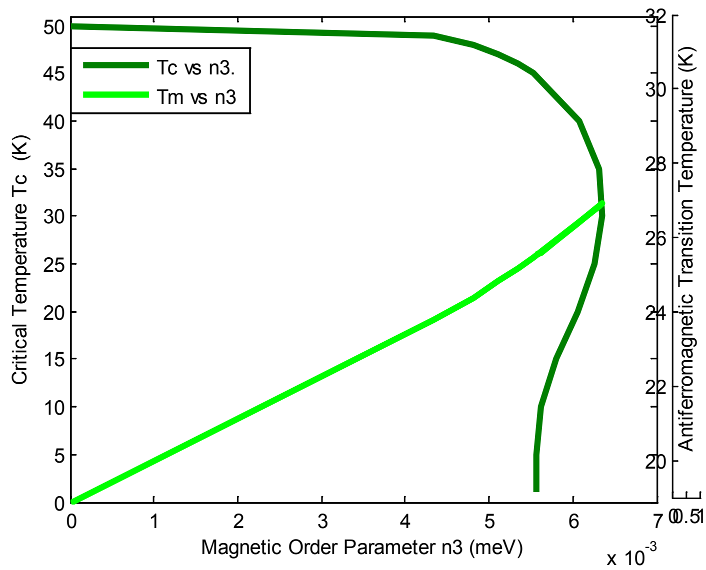

Figure 9. T_C and T_M (K) vs η_{33} (meV) for 3 band model.

A common notion that suggests superconductivity and magnetism to be hostile to each other, thus if this was the universal rule, then with T_C increasing, η should have decreased. In Figure 1, it is seen that till about a critical T_C of 9 K, both superconductivity and magnetism are seen to support each other, that is with increasing T_C, η also increases for this low value of T_C. The explanation for this kind of unusual trend can be reasoned out from the findings of L. Boeri *et al.* [43] that talks about electron-phonon coupling. A possible reason could be static magnetism [44] that is independent of doping and is seen to increase the electron phonon coupling constant λ, which in turn increases T_C. Also with a strong electron phonon coupling in this region, a strong electron electron interaction is seen in the Cooper pair that signifies both the orders to support each other and in no case superconductivity shows any signs of suppression. Beyond a certain doping, wherein doping can disturb static magnetism which makes λ start decreasing. This again makes T_C to decrease with increasing value of η. Thus a weak electron phonon coupling exists in this region, showing a weak electron-electron interaction in the Cooper pair that shows both the orders to be hostile to each other, signifying that superconductivity is suppressed.

Beyond the 9 K T_C region in **Figure 3**, at high values of T_C, η decreases which shows the usual trend. Similar kind of behaviour is seen in **Figure 4** and **Figure 7** for two and three band models respectively. The critical T_C for two band model is about 35 K and for the three band model is around 25 K.

Another probable reason for this kind of behaviour of T_C can be seen from the experimental findings of R. M. Fernandes *et al.* [45] that show how disorder affects the T_C of the s+− superconducting state in iron pnictides. In the underdoped region, superconductivity emerges from a pre-existing magnetic state and disorder gives rise to two competing effects, firstly breaking of the Cooper pairs, that reduces T_C and secondly suppression of the itinerant magnetic order that increases T_C. Their findings show that for a wide range of parameters in the coexistence state, T_C can increase with disorder.

In **Figure 2**, **Figure 5** and **Figure 8**, T_M vs η for one, two and three band models respectively is shown. It is observed that η increases with T_M. In the curves at a certain T_M, about 9 K for one band model, 11 K for two band model and 25 K for three band model, an abrupt slight increase in the value of η with T_M is seen. This unusual trend is attributed to the sharp peak that is observed in the specific heat curve due to AFM ordering of Sm^{3+} magnetic ions in the system which is otherwise not seen in the lanthanum compound that has non-magnetic La^{3+} ions [46].

Comparing the data of one, two and three band models, it is seen that with increasing number of bands, the coexistence region increases as is evident from the combined graph of T_C vs η and T_M vs η, thereby showing that the material can withhold a larger value of magnetic field upon increasing the number of bands.

4. Conclusions

Iron pnictides are a special class of superconductors. In the present research work, the doped samarium iron pnictide compound SmOFeAs is theoretically studied. Also earlier studies on the effect of multiband structure on critical temperature and electronic specific heat in SmOFeAs iron pnictide superconductor has been studied by Shamin Masih *et al.* [47]. In this research work, theoretical calculations are made uptil the three band model as Ummarino has suggested that a simple three band model in strong-coupling regime can reproduce in a quantitative way the experimental T_C. From the findings of R. M. Fernandes *et al.* on unconventional pairing in the iron arsenide superconductors, the results show theoretically that AFM and superconductivity can coexist in these materials only if Cooper pairs form an unconventional, sign-changing state. Also their study finds that AFM and conventional phonon-mediated superconductivity cannot coexist. Therefore unconventional s+− pairing is located near the borderline between phase coexistence and mutual exclusion. Their findings strongly suggest that superconductivity is unconventional in iron pnictides. This study further points out that correlation between superconductivity and magnetism doesn't change with increasing number of bands.

To conclude this work, one can say that the study has given insight into how these multiband structures behave and how the possibility for coexistence increases making the material more robust in nature. Attempt has been made to give explanations for both the regular and anomalous behaviors of the parameters under study.

Conflicts of Interest

The authors declare no conflicts of interest.

References

[1] Kamihara, Y., Hiramatsu, H., Hirano, M., Kawamura, R., Yanagi, H., Kamiya, T. and Hosono, H. (2006) Iron-Based Layered Superconductor: LaOFeP. *Journal of the American Chemical Society*, **128**, 10012-10013. https://doi.org/10.1021/ja063355c

[2] Kamihara, Y., Watanabe, T., Hirano, M. and Hosono, H. (2008) Iron-Based Layered Superconductor La[$O_{1-x}F_x$]FeAs (x = 0.05 - 0.12) with T_c = 26K. *Journal of the American Chemical Society*, **130**, 3296-3297. https://doi.org/10.1021/ja800073m

[3] Johnston, D.C. (2010) The Puzzle of High Temperature Superconductivity in Layered Iron Pnictides and Chalcogenides. *Advances in Physics*, **59**, 803-1061. https://doi.org/10.1080/00018732.2010.513480

[4] Bednorz, J.G. and Müller, K.A. (1986) Possible High T_c Superconductivity in the Ba-La-Cu-O System. *Zeitschrift für Physik B*, **64**, 189-193. https://doi.org/10.1007/BF01303701

[5] Ren, Z.A., Lu, W., Yang, J., *et al.* (2008) Superconductivity at 55K in Iron-Based F-Doped Layered Quaternary Compound Sm[$O_{1-x}F_x$]FeAs. *Chinese Physics Letters*, **25**, 2215-2216. https://doi.org/10.1088/0256-307X/25/6/080

[6] Chen, X., Dai, P., Feng, D., Xiang, T. and Zhang, F.C. (2014) Iron-Based High Transition Temperature Superconductors. *National Science Review*, **1**, 371-395. https://doi.org/10.1093/nsr/nwu007

[7] Oh, H., Moon, J., Shin, D., Moon, C.-Y. and Choi, H.J. (2011) Brief Review on Iron-Based Superconductors: Are There Clues for Unconventional Superconductivity? *Progress in Superconductivity*, **84**, 65-84.

[8] Tytarenko, A., Nakatsukasa, K., Huang, Y.K., Johnston, S. and Van Heumen, E. (2016) From Bad Metal to Kondo Insulator: Temperature Evolution of the Optical Properties of SmB_6. *New Journal of Physics*, **18**, Article ID: 123003. https://doi.org/10.1088/1367-2630/18/12/123003

[9] Nakajima, M., Ishida, S., Tanaka, T., Kihou, K., Tomioka, Y., Saito, T., Lee, C.H., Fukazawa, H., Kohori, Y., Kakeshita, T., Iyo, A., Ito, T., Eisaki, H. and Uchida, S.I. (2014) Strong Electronic Correlations in Iron Pnictides: Comparison of Optical Spectra for $BaFe_2As_2$-Related Compounds. *Journal of the Physical Society of Japan*,

83, Article ID: 104703. https://doi.org/10.7566/JPSJ.83.104703

[10] Yi, W., Sun, L., Ren, Z., Lu, W., Dong, X., Zhang, H.J., Dai, X., Fang, Z., Li, Z., Che, G., Yang, J., Shen, X., Zhou, F. and Zhao, Z. (2008) Pressure Effect on Superconductivity of Iron-Based Arsenic-Oxide $ReFeAsO_{0.85}$ (Re = Sm and Nd). *Europhysics Letters*, **83**, Article No. 57002. https://doi.org/10.1209/0295-5075/83/57002

[11] Kobayashi, K., Yamaura, J.I., Iimura, S., Maki, S., Sagayama, H., Kumai, R., Murakami, Y., Takahashi, H., Matsuishi, S. and Hosono, H. (2016) Pressure Effect on Iron-Based Superconductor $LaFeAsO_{1-x}H_x$: Peculiar Response of 1111-Type Structure. *Scientific Reports*, **6**, Article No. 39646. https://doi.org/10.1038/srep39646

[12] Wang, A.F., Xiang, Z.J., Ying, J.J., Yan, Y.J., Cheng, P., Ye, G.J., Luo, X.G. and Chen, X.H. (2012) Pressure Effects on the Superconducting Properties of Single-Crystalline Co-Doped NaFeAs. *New Journal of Physics*, **14**, Article ID: 113043. https://doi.org/10.1088/1367-2630/14/11/113043

[13] Igawa, K., Okada, H., Takahashi, H., Matsuishi, S., Kamihara, Y., Hirano, M., Hosono, H., Matsubayashi, K. and Uwatoko, Y. (2009) Pressure-Induced Superconductivity in Iron Pnictide Compound $SrFe_2As_2$. *Journal of the Physical Society of Japan*, **78**, 5-6. https://doi.org/10.1143/JPSJ.78.025001

[14] Ye, Z.R., Zhang, Y., Xie, B.P. and Feng, D.L. (2013) Angle-Resolved Photoemission Spectroscopy Study on Iron-Based Superconductors. *Chinese Physics B*, **22**, Article ID: 087407. https://doi.org/10.1088/1674-1056/22/8/087407

[15] Laad, M.S. and Craco, L. (2009) Theory of Multiband Superconductivity in Iron Pnictides. *Physical Review Letters*, **103**, Article ID: 017002. https://doi.org/10.1103/PhysRevLett.103.017002

[16] Nomura, T. (2008) Possibility of Unconventional Pairing Due to Coulomb Interaction in Fe-Based Pnictide Superconductors: Perturbative Analysis of Multi-Band Hubbard Models. *Journal of the Physical Society of Japan*, **77**, 123-124. https://doi.org/10.1143/JPSJS.77SC.123

[17] Hu, J., Liu, T.J., Qian, B., Rotaru, A., Spinu, L. and Mao, Z.Q. (2011) Calorimetric Evidence of Strong-Coupling Multiband Superconductivity in $Fe(Te_{0.57}Se_{0.43})$ Single Crystal. *Physical Review B*, **83**, Article ID: 134521. https://doi.org/10.1103/PhysRevB.83.134521

[18] Terashima, K., Sekiba, Y., Bowen, J.H., Nakayama, K., Kawahara, T., Sato, T., Richard, P., Xu, Y.M., Li, L.J., Cao, G.H., Xu, Z.A., Ding, H. and Takahashi, T. (2009) Fermi Surface Nesting Induced Strong Pairing in Iron-Based Superconductors. *Proceedings of the National Academy of Sciences of the United States of America*, **106**, 7330-7333. https://doi.org/10.1073/pnas.0900469106

[19] Ajay, R.L. (2013) Electronic Spectra of Iron Pnictide Superconductors: Influence of Multi-Orbitals Hopping and Hund's Coupling. *Journal of Superconductivity and Novel Magnetism*, **26**, 527-538. https://doi.org/10.1007/s10948-012-1780-1

[20] Podolsky, D. (2012) Untangling the Orbitals in Iron-Based Superconductors. *Physics* (*College. Park. Md*), **5**, 61. https://doi.org/10.1103/Physics.5.61

[21] Raghu, S., Qi, X.L., Liu, C.X., Scalapino, D.J. and Zhang, S.C. (2008) Minimal Two-Band Model of the Superconducting Iron Oxypnictides. *Physical Review B*: *Condensed Matter and Materials Physics*, **77**, Article ID: 220503. https://doi.org/10.1103/PhysRevB.77.220503

[22] Frank, S.S., Kumar, A., Khandka, S. and Masih, S. (2015) Thermodynamical Properties of LiFeAs Superconductor Using Two Band Model. *International Journal of Engineering Sciences & Research Technology*, **4**, 480-487.

[23] Nuwal, A., Kakani, S. and Kakani, S.L. (2014) Two Band Model for the Iron Based

Superconductors. *Indian Journal of Pure & Applied Physics*, **52**, 411-422.

[24] Maksimov, E.G., Karakozov, A.E., Gorshunov, B.P., Prokhorov, A.S., Voronkov, A.A., Zhukova, E.S., Nozdrin, V.S., Zhukov, S.S., Wu, D., Dressel, M., Haindl, S., Iida, K. and Holzapfel, B. (2011) Two-Band Bardeen-Cooper-Schrieffer Superconducting State of the Iron Pnictide Compound $Ba(Fe_{0.9}Co_{0.1})_2As_2$. *Physical Review B: Condensed Matter and Materials Physics*, **83**, Article ID: 140502.

[25] Stanev, V. and Tešanović, Z. (2010) Three-Band Superconductivity and the Order Parameter That Breaks Time-Reversal Symmetry. *Physical Review B: Condensed Matter and Materials Physics*, **81**, Article ID: 134522. https://doi.org/10.1103/PhysRevB.81.134522

[26] Daghofer, M., Nicholson, A., Moreo, A. and Dagotto, E. (2010) Three Orbital Model for the Iron-Based Superconductors. *Physical Review B: Condensed Matter and Materials Physics*, **81**, Article ID: 014511. https://doi.org/10.1103/PhysRevB.81.014511

[27] Lee, P.A. and Wen, X.G. (2008) Spin-Triplet p-Wave Pairing in a Three-Orbital Model for Iron Pnictide Superconductors. *Physical Review B: Condensed Matter and Materials Physics*, **78**, Article ID: 144517. https://doi.org/10.1103/PhysRevB.78.144517

[28] Ummarino, G.A., Tortello, M., Daghero, D. and Gonnelli, R.S. (2009) Three-Band s± Eliashberg Theory and the Superconducting Gaps of Iron Pnictides. *Physical Review B: Condensed Matter and Materials Physics*, **80**, Article ID: 172503. https://doi.org/10.1103/PhysRevB.80.172503

[29] Benfatto, L., Capone, M., Caprara, S., Castellani, C. and Di Castro, C. (2008) Multiple Gaps and Superfluid Density from Interband Pairing in a Four-Band Model of the Iron Oxypnictides. *Physical Review B: Condensed Matter and Materials Physics*, **78**, 140502(R). https://doi.org/10.1103/PhysRevB.78.140502

[30] Singh, D.J. (2012) Magnetism and Superconductivity in Iron Pnictides. *Acta Physica Polonica A*, **121**, 999-1004. https://doi.org/10.12693/APhysPolA.121.999

[31] Vorontsov, A.B., Vavilov, M.G. and Chubukov, A.V. (2009) Interplay between Magnetism and Superconductivity in the Iron Pnictides. *Physical Review B: Condensed Matter and Materials Physics*, **79**, 060508(R). https://doi.org/10.1103/PhysRevB.79.060508

[32] Kordyuk, A.A. (2012) Iron-Based Superconductors: Magnetism, Superconductivity, and Electronic Structure. *Low Temperature Physics*, **38**, 888-899. https://doi.org/10.1063/1.4752092

[33] Zhigadlo, N.D., Weyeneth, S., Katrych, S., Moll, P.J.W., Rogacki, K., Bosma, S., Puzniak, R., Karpinski, J. and Batlogg, B. (2012) High-Pressure Flux Growth, Structural, and Superconducting Properties of LnFeAsO (Ln = Pr, Nd, Sm) Single Crystals. *Physical Review B: Condensed Matter and Materials Physics*, **86**, Article ID: 214509.

[34] Fernandes, R.M., Pratt, D.K., Tian, W., Zarestky, J., Kreyssig, A., Nandi, S., Kim, M.G., Thaler, A., Ni, N., Canfield, P.C., McQueeney, R.J., Schmalian, J. and Goldman, A.I. (2010) Unconventional Pairing in the Iron Arsenide Superconductors. *Physical Review B: Condensed Matter and Materials Physics*, **81**, 29-33. https://doi.org/10.1103/PhysRevB.81.140501

[35] Lu, X.F., Wang, N.Z., Wu, H., Wu, Y.P., Zhao, D., Zeng, X.Z., Luo, X.G., Wu, T., Bao, W., Zhang, G.H., Huang, F.Q., Huang, Q.Z. and Chen, X.H. (2015) Coexistence of Superconductivity and Antiferromagnetism in $(Li_{0.8}Fe_{0.2})OHFeSe$. *Nature Materials*, **14**, 325-329. https://doi.org/10.1038/nmat4155

[36] Mebrahtu, A. and Singh, P. (2015) Coexistence of Superconductivity and Antifer-

romagnetism in $SmAsO_{1-x}F_xFe$. *World Journal of Condensed Matter Physics*, **5**, 138-147. https://doi.org/10.4236/wjcmp.2015.53016

[37] Afrassa, M.A. and Singh, P. (2014) Theoretical Study of the Interplay of Superconductivity and Magnetism in FeAs Based Superconductors. *World Journal of Condensed Matter Physics*, **4**, 53-57. https://doi.org/10.4236/wjcmp.2014.42008

[38] Desta, T., Kahsay, G. and Singh, P. (2017) Theoretical Analyses of Superconductivity in Iron Based Superconductor $Ba_{1-x}K_xFe_2As_2$. *Momona Ethiopian Journal of Science*, **9**, 134. https://doi.org/10.4314/mejs.v9i2.1

[39] Singh, P. (2011) Coexistence of Superconductivity and Ferromagnetism. *Journal of Superconductivity and Novel Magnetism*, **24**, 945-949. https://doi.org/10.1007/s10948-010-0889-3

[40] Masih, S., Masih, P. and Khandka, S. (2018) Coexistence of Superconducting and Magnetic Order in One Band and Two Band SmOFeAs Superconductor. *Journal of Emerging Technologies and Innovative Research* (*JETIR*), **5**, 432-437.

[41] Zubarev, D.N. (1960) Double-Time Green Functions in Statistical Physics. *Soviet Physics Uspekhi*, **3**, 320-345. https://doi.org/10.1070/PU1960v003n03ABEH003275

[42] Ryan, D.H., Cadogan, J.M., Ritter, C., Canepa, F., Palenzona, A. and Putti, M. (2009) Coexistence of Long-Ranged Magnetic Order and Superconductivity in the Pnictide Superconductor $SmFeAsO_{1-x}F_x$ (x = 0, 0.15). *Physical Review B*: *Condensed Matter and Materials Physics*, **80**, 220503(R). https://doi.org/10.1103/PhysRevB.80.220503

[43] Boeri, L., Calandra, M., Mazin, I.I., Dolgov, O.V. and Mauri, F. (2010) Effects of Magnetism and Doping on the Electron-Phonon Coupling in $BaFe_2As_2$. *Physical Review B*: *Condensed Matter and Materials Physics*, **82**, 020506(R). https://doi.org/10.1103/PhysRevB.82.020506

[44] Drew, A.J., Niedermayer, C., Baker, P.J., Pratt, F.L., Blundell, S.J., Lancaster, T., Liu, R.H., Wu, G., Chen, X.H., Watanabe, I., Malik, V.K., Dubroka, A., Rössle, M., Kim, K.W., Baines, C. and Bernhard, C. (2009) Coexistence of Static Magnetism and Superconductivity in $SmFeAsO_{1-x}F_x$ as Revealed by Muon Spin Rotation. *Nature Materials*, **8**, 310-314. https://doi.org/10.1038/nmat2396

[45] Fernandes, R.M., Vavilov, M.G. and Chubukov, A.V. (2012) Enhancement of T_c by Disorder in Underdoped Iron Pnictide Superconductors. *Physical Review B*: *Condensed Matter and Materials Physics*, **85**, 140512(R). https://doi.org/10.1103/PhysRevB.85.140512

[46] Ding, L., He, C., Dong, J.K., Wu, T., Liu, R.H., Chen, X.H. and Li, S.Y. (2008) Specific Heat of the Iron-Based High-T_c Superconductor $S_mO_{1-x}F_xFeAs$. *Physical Review B*: *Condensed Matter and Materials Physics*, **77**, 180510(R).

[47] Masih, S., Masih, P. and Khandka, S. (2022) Theoretical Study on the Effect of Multiband Structure on Critical Temperature and Electronic Specific Heat in SmOFeAs Iron Pnictide Superconductor. *Journal of Applied Mathematics and Physics*, **10**, 2232-2244. https://doi.org/10.4236/jamp.2022.107153